

energies for the process  $\text{CH}_3\text{X}^{*+} \rightarrow \text{CH}_3\text{X}^{2+}$  are considerably higher than the  $Q_{\text{min}}$  values obtained through charge stripping of  $\text{CH}_3\text{X}^{*+}$  cations.<sup>51</sup>

Comparison of the experimental  $Q_{\text{min}}$  values with the calculated ionization energies shows moderate (though by no means perfect) agreement for the ylide dications  $\text{CH}_2\text{XH}^{2+}$  when  $\text{X} = \text{OH}$  ( $Q_{\text{min}} = 16.5$  eV,  $\text{IE}_v = 16.7$  eV,  $\text{IE}_a = 15.6$  eV),  $\text{X} = \text{F}$  ( $Q_{\text{min}} = 17.9$  eV,  $\text{IE}_v = 18.8$  eV,  $\text{IE}_a = 17.6$  eV), and  $\text{X} = \text{Cl}$  ( $Q_{\text{min}} = 17.5$  eV,  $\text{IE}_v = 17.2$  eV,  $\text{IE}_a = 16.1$  eV). However, there are major discrepancies for  $\text{X} = \text{NH}_2$  ( $Q_{\text{min}} = 18.9$  eV,  $\text{IE}_v = 16.2$  eV,  $\text{IE}_a = 15.9$  eV) and  $\text{X} = \text{SH}$  ( $Q_{\text{min}} = 19.8$  eV,  $\text{IE}_v = 15.7$  eV,  $\text{IE}_a = 15.5$  eV). The theoretical values in these two instances are supported by EOM calculations and by higher level conventional calculations. Thus, for  $\text{X} = \text{NH}_2$  the calculated  $\text{IE}_v$  values are 16.2 (MP3/6-31G\*\*), 16.2 (MP4/6-31G\*\*), 15.8 (EOM/6-31G\*\*), and 16.3 eV (MP3/6-311G\*\*) compared with the experimental  $Q_{\text{min}}$  of 18.9 eV, while for  $\text{X} = \text{SH}$  the calculated  $\text{IE}_v$  values are 15.7 (MP3/6-31G\*\*) and 15.4 eV (EOM/6-31G\*\*) compared with the experimental  $Q_{\text{min}}$  value of 19.8 eV. The disagreement between theory and experiment is sufficiently large that reinterpretation of the experimental data could be in order.

Finally, we note that the significant differences between  $\text{IE}_v$  and  $\text{IE}_a$  values for a number of systems ( $\text{X} = \text{OH}$ ,  $\text{F}$ ,  $\text{PH}_2$ , and

$\text{Cl}$ ) reflect a marked difference between the geometry of the ylidion ( $\text{CH}_2\text{XH}^+$ ) and the ylide dication ( $\text{CH}_2\text{XH}^{2+}$ ) in these cases. This effect would not, however, account for the discrepancy noted above between the theoretical and experimental ionization energies.

### Concluding Remarks

Ylide dications ( $\text{CH}_2\text{XH}^{2+}$ ), although thermodynamically unstable with respect to fragmentation products, are found to lie in moderately deep potential wells and should be observable species. In contrast, their conventional isomers ( $\text{CH}_3\text{X}^{2+}$ ) can rearrange or fragment with little or no barrier. The calculated ionization energies corresponding to production of ylide dications from ylidions are generally in moderate agreement with experimental  $Q_{\text{min}}$  values. However, there are a number of discrepancies, and a reexamination of the experimental data is suggested in these cases. The calculations indicate that production of  $\text{CH}_3\text{X}^{2+}$  dications from  $\text{CH}_3\text{X}^{*+}$  is a high-energy process, and the experimental  $Q_{\text{min}}$  values for such systems are likely to correspond to production of the isomeric  $\text{CH}_2\text{XH}^{2+}$  dications.

Registry No.  $\text{CH}_2\text{NH}_3^{2+}$ , 103884-69-1;  $\text{CH}_3\text{NH}_2^{2+}$ , 103958-76-5;  $\text{CH}_2\text{OH}_2^{2+}$ , 83584-97-8;  $\text{CH}_3\text{OH}^{2+}$ , 99674-12-1;  $\text{CH}_2\text{FH}_2^{2+}$ , 103751-46-8;  $\text{CH}_2\text{F}_2^{2+}$ , 103958-74-3;  $\text{CH}_2\text{PH}_2^{2+}$ , 103884-70-4;  $\text{CH}_3\text{PH}_2^{2+}$ , 103958-77-6;  $\text{CH}_2\text{SH}_2^{2+}$ , 103884-71-5;  $\text{CH}_3\text{SH}^{2+}$ , 103958-75-4;  $\text{CH}_2\text{ClH}^{2+}$ , 103884-72-6;  $\text{CH}_3\text{Cl}^{2+}$ , 103958-73-2;  $\text{Ph}_2^{*+}$ , 12339-26-3;  $\text{Ph}_3^{*+}$ , 29724-05-8;  $\text{CH}_2\text{PH}_2^+$ , 59025-96-6;  $\text{HCPH}_2^{*+}$ , 98077-14-6;  $\text{CH}_2\text{PH}^{*+}$ , 89387-22-4;  $\text{SH}^+$ , 12273-42-6;  $\text{SH}_2^{*+}$ , 77544-69-5;  $\text{CH}_2\text{SH}^+$ , 54043-03-7;  $\text{HCSH}^{*+}$ , 61356-81-8;  $\text{Cl}^+$ , 24203-47-2;  $\text{ClH}^{*+}$ , 12258-94-5;  $\text{CH}_2\text{Cl}^+$ , 59000-00-9;  $\text{HCCl}^+$ , 89877-51-0;  $\text{HCCl}_2^+$ , 103904-09-2;  $\text{CH}_2^{*+}$ , 15091-72-2;  $\text{H}_2$ , 1333-74-0;  $\text{H}_2^{*+}$ , 12184-90-6;  $\text{CH}_3^+$ , 14531-53-4.

(51) Further information on the stabilities and lifetimes of the  $\text{CH}_3\text{X}^{2+}$  species might be obtained from state of the art photoionization or Auger spectroscopy experiments.

(52) The 6-311G\*\* basis set is described in: Krishnan, R.; Binkley, J. S.; Seeger, R.; Pople, J. A. *J. Chem. Phys.* 1980, 72, 650.

## A MCSCF Study of Homoaromaticity and the Role of Ion Pairing in the Stabilization of Carbanions

Roland Lindh,\*† Björn O. Roos,† Göran Jonsäll,† and Per Ahlberg\*‡

Contribution from the Department of Theoretical Chemistry, University of Lund, Chemical Centre, S-221 00 Lund, Sweden, and the Department of Organic Chemistry, University of Göteborg, S-412 96 Göteborg, Sweden. Received March 17, 1986

**Abstract:** The bicyclo[3.2.1]octa-3,6-dien-2-yl anion (I), the anion I lithium cation complex, the allyl anion (X), the allyl radical, the allyl anion lithium cation complex, the ethene molecule, and the ethene lithium cation complex have been studied by means of multiconfigurational SCF (MCSCF) and analytical gradients. The calculations have been confined to minimal and split-valence basis sets. The large distance between the  $\text{C}_2$  olefinic bridge and the  $\text{C}_3$  carbanionic bridge of anion I and the short  $\text{C}_6$ - $\text{C}_7$  bond distance imply bishomoaromaticity to be negligible. According to these results, homoaromaticity is not responsible for the observed stability in many potentially homoaromatic carbanions. The stability of anion I in the gas phase is instead explained in terms of a simple electrostatic model, where the quadrupole moment in the  $\text{C}_2$  olefinic bridge stabilizes the charge in the  $\text{C}_3$  carbanionic bridge. This model agrees quantitatively with experiment. Calculations on the anion I lithium cation complex showed that in solution an additional attractive interaction between the  $\text{C}_2$  olefinic bridge and the lithium cation can contribute. This additional interaction is estimated to stabilize the carbanion-lithium ion pair in the gas phase by about 16 kcal/mol. However, the stabilizing interactions of anion I in solution (quadrupole-charge and counterion-anion interactions) will be reduced by solvent shielding. The relative ratios of the different stabilizing interactions are therefore difficult to estimate. The geometrical findings of this paper have been verified by a recent X-ray experiment.

The concept of homoaromaticity has been controversial since it was introduced by Winstein almost 30 years ago.<sup>1</sup> Although homoaromatic stabilization of carbocations is well established,<sup>2</sup> more recent work concludes that homoaromaticity is not expected to be of importance in carbanions and neutral compounds, including radicals.<sup>3</sup> This conclusion about carbanions is based upon

theoretical studies of the prototype of bishomoaromatic anions, i.e., the bicyclo[3.2.1]octa-3,6-dien-2-yl anion (I),<sup>4</sup> and other

(1) (a) Applequist, D. E.; Roberts, J. D. *J. Am. Chem. Soc.* 1956, 78, 4012. (b) Winstein, S. *J. Am. Chem. Soc.* 1959, 81, 6524. For reviews, see: (c) Winstein, S. *Q. Rev., Chem. Soc.* 1969, 23, 141. Winstein, S. *Spec. Publ.—Chem. Soc.* 1967, 21, 5. (d) Winstein, S. *Carbanion Ions*; Olah, G. A., Schleyer, P. v. R., Eds.; Wiley: New York, 1972; Vol. 3, Chapter 22, p 965. (e) Paquette, L. A. *Angew. Chem., Int. Ed. Engl.* 1978, 17, 106. (f) Warner, P. M. *Top. Nonbenzenoid Aromat. Chem.* 1976, 2.

\*University of Lund.

†University of Göteborg.

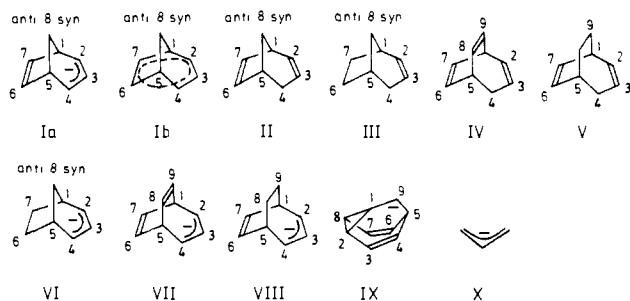


Figure 1. Some relevant structures.

related ions (Figure 1) by Grutzner and Jorgensen using semiempirical MINDO/3 and ab initio STO-3G calculations<sup>5a</sup> and by Kaufmann et al. using semiempirical MNDO and ab initio STO-3G methods.<sup>5b</sup> In response to this work, Brown et al.,<sup>5c</sup> studied the interaction of an allyl anion with ethene by ab initio STO-3G methods. On the basis of their results they refute the claims by Grutzner and Jorgensen and Kaufmann et al.<sup>5a,b</sup> However, the results of Brown et al. are based on observations

(2) (a) Olah, G. A.; Staral, J. S.; Liang, G. *J. Am. Chem. Soc.* **1974**, *96*, 6233. (b) Olah, G. A.; Staral, J. S.; Spear, R. J.; Liang, G. *J. Am. Chem. Soc.* **1975**, *97*, 5489. (c) Winstein, S.; Kaesz, H. D.; Kreiter, C. G.; Friedrich, E. C. *J. Am. Chem. Soc.* **1965**, *87*, 3267. (d) Warner, P.; Harris, D. L.; Bradley, C. H.; Winstein, S. *Tetrahedron Lett.* **1970**, 4013. (e) Winstein, S.; Kreiter, C. G.; Brauman, J. I. *J. Am. Chem. Soc.* **1966**, *88*, 2047. (f) Oth, J. F. M.; Smith, D. M.; Prange, U.; Schröder, G. *Angew. Chem., Int. Ed. Engl.* **1973**, *12*, 327. (g) Paquette, L. A.; Broadhurst, M. J.; Warner, P.; Olah, G. A.; Liang, G. *J. Am. Chem. Soc.* **1973**, *95*, 3386. (h) Winstein, S.; Shatavsky, M.; Norton, C.; Woodward, R. B. *J. Am. Chem. Soc.* **1955**, *77*, 4183. (i) Winstein, S.; Shatavsky, M. *J. Am. Chem. Soc.* **1956**, *78*, 592. (j) Winstein, S.; Hansen, R. L. *Tetrahedron Lett.* **1960**, 4, 25. (k) Gassman, P. G.; Patton, D. S. *J. Am. Chem. Soc.* **1969**, *91*, 2160. (l) Lustgarten, R. K.; Brookhart, M.; Winstein, S.; Gassman, P. G.; Patton, D. S.; Richey, H. G., Jr.; Nichols, J. D. *Tetrahedron Lett.* **1970**, 1699. (m) Ahlberg, P.; Harris, D. L.; Roberts, M.; Warner, P.; Seidl, P.; Sakai, M.; Cook, D.; Diaz, A.; Dirlam, J. P.; Hamberger, H.; Winstein, S. *J. Am. Chem. Soc.* **1972**, *94*, 7063 and references therein. (n) Engdahl, C.; Ahlberg, P. *J. Chem. Res., Synop.* **1977**, 342. (o) Huang, M. B.; Goscinski, O.; Jonsäll, G.; Ahlberg, P. *J. Chem. Soc., Perkin Trans. 2* **1983**, 305. (p) Jonsäll, G.; Ahlberg, P. *J. Am. Chem. Soc.*, **1986**, *108*, 3819. (q) Winstein, S.; Sonnenberg, J.; de Vries, L. *J. Am. Chem. Soc.* **1959**, *81*, 6523. (r) Winstein, S.; Sonnenberg, J. *J. Am. Chem. Soc.* **1961**, *83*, 3235. (s) Winstein, S.; Friedrich, E. C.; Baker, R.; Lin, Y. *Tetrahedron, Suppl.* **1966**, *8*, 621. (t) Masamune, S.; Sakai, M.; Kemp-Jones, A. V.; Nakashima, T. *Can. J. Chem.* **1974**, *52*, 855. (u) Coates, R. M.; Fretz, E. R. *J. Am. Chem. Soc.* **1975**, *97*, 2538. (v) Olah, G. A.; Surya Prakash, G. K.; Rawdah, T. N.; Whittaker, D.; Rees, J. C. *J. Am. Chem. Soc.* **1979**, *101*, 3935.

(3) (a) Kao, J.; Radom, L.; *J. Am. Chem. Soc.* **1978**, *100*, 760. (b) Houk, K. N.; Gaudour, R. W.; Strozler, R. W.; Rondan, N. G.; Paquette, L. A. *J. Am. Chem. Soc.* **1979**, *101*, 6797. (c) Olah, G. A.; Asensio, G.; Mayr, H.; Schleyer, P. v. R. *J. Am. Chem. Soc.* **1978**, *100*, 4347. (d) Christoph, G. G.; Muthard, J. L.; Paquette, L. A.; Boehm, M. C.; Gleiter, R. *J. Am. Chem. Soc.* **1978**, *100*, 7782. (e) Paquette, L. A.; Kukla, M. J.; Ley, S. V.; Traynor, S. G. *J. Am. Chem. Soc.* **1977**, *99*, 4756. (f) Sustman, R.; Geilert, R. W.; *Chem. Ber.* **1978**, *111*, 42. (g) Trimitsis, G. B.; Tuncay, A. *J. Am. Chem. Soc.* **1976**, *98*, 1997. (h) Trimitsis, G. B.; Tuncay, A. *J. Am. Chem. Soc.* **1975**, *97*, 7193. (i) Trimitsis, G. B.; Zimmerman, P. *J. Chem. Soc., Chem. Commun.* **1984**, 1506. (j) Kawamura, T.; Takeichi, Y.; Hayashida, S.; Sakamoto, M.; Yonezawa, T. *Bull. Chem. Soc. Jpn.* **1978**, *51*, 3069.

(4) Brown, J. M.; Ocolowitz, J. L. *Chem. Commun.* **1965**, 376. (b) Brown, J. M.; Ocolowitz, J. L. *J. Chem. Soc. B* **1968**, 411. (c) Brown, J. M. *Chem. Commun.* **1967**, 638. (d) Winstein, S.; Ogliaruso, M.; Sakai, M.; Nicholson, J. M. *J. Am. Chem. Soc.* **1967**, *89*, 3656. (e) Moncur, M. V.; Grutzner, J. B. *J. Am. Chem. Soc.* **1973**, *95*, 6449. (f) Köhler, F. H.; Hertkorn, N. *Chem. Ber.* **1983**, *116*, 3274. (g) Christl, M.; Leininger, H.; Brückner, D. *J. Am. Chem. Soc.* **1983**, *105*, 4843. For experimental studies of related anions, see: (h) Rosenthal, J. W.; Winstein, S. *Tetrahedron Lett.* **1970**, 2683. (i) Brown, J. M.; Cain, E. N.; McIvor, M. C. *J. Chem. Soc. B* **1971**, 730. (j) Goldstein, M. J.; Natowsky, S. *J. Am. Chem. Soc.* **1973**, *95*, 6451. (k) Staley, S. W.; Reichard, D. W. *J. Am. Chem. Soc.* **1969**, *91*, 3998. (l) Christl, M.; Brückner, D. *Chem. Ber.* **1986**, *119*, 2025.

(5) (a) Grutzner, J. B.; Jorgensen, W. L. *J. Am. Chem. Soc.* **1981**, *103*, 1372. (b) Kaufmann, E.; Mayr, H.; Chandrasekhar, J.; Schleyer, P. v. R. *J. Am. Chem. Soc.* **1981**, *103*, 1375. (c) Brown, J. M.; Elliott, R. J.; Richards, W. G. *J. Chem. Soc., Perkin Trans. 2* **1982**, 485. For other earlier and related work, see: (d) Goldstein, M. J. *J. Am. Chem. Soc.* **1967**, *89*, 6357. (e) Goldstein, M. J.; Hoffmann, R. *J. Am. Chem. Soc.* **1971**, *93*, 6193. (f) Hehre, W. J. *J. Am. Chem. Soc.* **1972**, *94*, 8908; **1973**, *95*, 5807; **1974**, *96*, 5207. (g) Haddon, R. C. *J. Am. Chem. Soc.* **1975**, *97*, 3608. (h) Jorgensen, W. L. *J. Am. Chem. Soc.* **1976**, *98*, 6784. (e) Haddon, R. C. *J. Org. Chem.* **1979**, *44*, 3608.

Table I. Number of Primitive and Contracted Basis Functions in the Different Calculations

complex	primitive functions	contracted functions
Minimal Basis		
C <sub>2</sub> H <sub>4</sub>	48	14
C <sub>3</sub> H <sub>5</sub> <sup>-</sup>	69	20
LiC <sub>3</sub> H <sub>5</sub>	84	25
C <sub>8</sub> H <sub>9</sub> <sup>-</sup>	171	49
LiC <sub>8</sub> H <sub>9</sub>	186	54
Split-Valence Basis		
C <sub>2</sub> H <sub>4</sub>	66	26
C <sub>3</sub> H <sub>5</sub> , C <sub>3</sub> H <sub>5</sub> <sup>-</sup>	95	37
LiC <sub>3</sub> H <sub>5</sub>	117	46
C <sub>8</sub> H <sub>9</sub> <sup>-</sup>	236	90
LiC <sub>8</sub> H <sub>9</sub>	258	99

of the allyl anion ethene complex within the repulsive region.

In the present paper we report results on anion I obtained with ab initio methods at a higher level of theory than previously reported. The complete active space SCF (CASSCF) method with minimal and split-valence basis sets was employed. Our results confirm the conclusions reached by Grutzner and Jorgensen and by Kaufmann et al. about the absence of homoaromaticity in carbanions. The interactions between unoccupied and occupied orbitals necessary to achieve homoaromaticity and bicycloaromaticity do not take place due to the large distance between the interacting bridges. The dominant interaction at the equilibrium distance is rather electrostatic interaction.

These illuminating theoretical results force us to look for alternative explanations for a large body of experimental results. Among these are the 10<sup>4.5</sup> times faster H/D exchange of hydrocarbon in II relative to III in dimethyl sulfoxide (Me<sub>2</sub>SO) containing KOBu-*t* and similar results obtained with other systems.<sup>4a,b</sup> What causes the δ 2,3 downfield <sup>1</sup>H NMR shift of the C<sub>6</sub> and C<sub>7</sub> hydrogens of anion I relative to the corresponding hydrogens in II if delocalization of negative charge is not responsible?<sup>4c-e</sup> Similarly, what causes the δ 43.8 upfield <sup>13</sup>C NMR shift of the C<sub>6</sub> and C<sub>7</sub> carbons of anion I relative to the corresponding carbons of II?<sup>4f,g</sup> Furthermore, in a recent paper, Washburn reports some challenging results. He has measured pK<sub>a</sub> values of compounds II, III, IV, and V in cyclohexylamine using cesium cyclohexylamide.<sup>6</sup> Anion I is found to be >12.2 kcal/mol more stabilized than anion VI, and ions VII and VIII are stabilized by their C<sub>2</sub> olefinic bridges by >11.4 and >8.7 kcal/mol, respectively. Washburn considers his results to be the first quantification of anionic homoaromatic stabilization.<sup>6</sup>

We have recently explored the possibility of using <sup>13</sup>C-<sup>13</sup>C coupling constants as structural probes for carbocations as well as carbanions. These results and isotopic perturbation studies gave no evidence for aromaticity in ion VII.<sup>2b,7</sup> Furthermore, in studies of the rearrangement mechanism of ion VII, by which the carbons in the ion are scrambled and which possibly makes use of the 9-barbaralyl anion IX as an intermediate, the counteranion is found to strongly influence the reactivity. Thus the lithium salt of VII in tetrahydrofuran (THF) was found to rearrange about 10<sup>2</sup> times faster than the corresponding potassium salt.<sup>7</sup> These results indicate that the anions investigated are not free anions but rather are paired with alkali cations. They are, therefore, most likely present as contact ion pairs in the solutions. That ion pairs may be the cause of the unusual stabilization and other observations made with potentially homoaromatic anions seems to have been ignored.

We now also wish to report CASSCF calculations of anion I and the allyl anion (X) paired with lithium ions. The results indicate a previously overlooked attraction between the lithium cation and the C<sub>2</sub> olefinic bridge in addition to the lithium cation C<sub>3</sub> carbanionic bridge interaction. The attractive interaction between the C<sub>2</sub> olefinic bridge and the lithium ion in solution and the stabilization of the C<sub>3</sub> carbanionic bridge by the quadrupole

(6) Washburn, W. N. *J. Org. Chem.* **1983**, *48*, 4287.

(7) Jonsäll, G.; Ahlberg, P. *J. Chem. Soc., Perkin Trans. 2*, in press.

Table II. Wave Function Parameters and Number of Configurations

complex	spin	symmetry	inactive orbitals <sup>a</sup> active orbitals	active electrons	configurations
C <sub>2</sub> H <sub>4</sub>	1	A <sub>g</sub> (D <sub>2h</sub> )	3 2 0 0 2 1 0 0 0 0 1 0 0 0 1 0	2	2
C <sub>3</sub> H <sub>5</sub>	2	A <sub>2</sub> (C <sub>2v</sub> )	6 4 0 0 0 0 2 1	3	4
C <sub>3</sub> H <sub>5</sub> <sup>-</sup>	1	A <sub>1</sub> (C <sub>2v</sub> )	6 4 0 0 0 0 2 1	4	4
LiC <sub>3</sub> H <sub>5</sub>	1	A'(C <sub>s</sub> )	7 4 4 2	4	57
C <sub>8</sub> H <sub>9</sub> <sup>-</sup>	1	A'(C <sub>s</sub> )	16 10 3 2	6	28
LiC <sub>8</sub> H <sub>9</sub>	1	A'(C <sub>s</sub> )	17 10 5 3	6	606

<sup>a</sup>Irreducible representations according to MOLECULE, see ref 13.

moment of the C<sub>2</sub> olefinic bridge may be the major causes for the unusual stability of the anion, rather than homoaromaticity.

### Method of Calculation

**Basis Sets.** The choice of basis sets in the case of anion I was very straightforward. The number of atoms and the low symmetry of anion I (C<sub>s</sub>) do not warrant the use of a basis set of a higher level of sophistication. We thus used two kinds of basis sets, a minimal basis and a split-valence basis. These basis sets will give us bond distances which may differ from experimental bond distances. However, the behavior of the minimal basis and the split-valence basis is well documented, and any deviations due to artifacts of the basis sets are well-known (too long CH bond distances of minimal basis, etc.). Therefore, calculations with minimal and split-valence basis sets will give us desirable accuracy.

The minimal basis of Roos et al.<sup>8</sup> was chosen. The basis was contracted as C(7s3p/2s1p) and Li(7s/2s). To the lithium basis were added p-type functions with exponents 0.1474 and 0.0596 and coefficients 1.926 50 and 3.220 82. The resulting basis was contracted as Li(7s2p/2s1p). The basis function of H was chosen to be the one of Huzinaga,<sup>9</sup> contracted as H(3s/1s). The split-valence basis was chosen to be the same as that of Huzinaga<sup>9</sup> and Dunning.<sup>10</sup> The split-valence basis was contracted as C(9s5p/3s2p), Li(9s4p/3s2p), and H(4s/2s). These choices of basis functions will give us the number of primitive and contracted basis functions as presented in Table I.

**CASSCF Approximation.** The complete active space SCF (CASSCF) method has been described in detail elsewhere,<sup>11,12</sup> and only a brief review of the method will therefore be given here. The CASSCF approach is a special form of the MCSCF method, where the orbital space is divided into three subspaces: inactive, active, and secondary orbitals. The inactive orbitals are taken to be doubly occupied in all configurations. It should be recalled that in the CASSCF method the inactive space is not a fixed core, since the doubly occupied orbitals are also optimized. The remaining electrons occupy the active orbitals, and the wave function comprises all the configurations, which can be formed by distributing these electrons among the active orbitals in all possible ways, consistent with a given overall spin and space symmetry.

The choice of the active space in a study of aromaticity of a molecule should be, if possible, all orbitals which constitute the  $\pi$  system of the molecule. We will adopt the same principles in this paper. Hence, the choice for ethene, allyl radical, and allyl anion (X) will be the bonding and the antibonding  $\pi$  orbitals, and in the two latter cases, we will also include the nonbonding  $\pi$  orbital (see Table II). For anion I the choice of active orbitals will resemble the active space of ethene and allyl anion (X).

It has been argued that cations can lend their p orbitals to anion I, so that the interaction in the aromatic system can be enhanced. Thus, in the calculations where the lithium cation is involved the p orbitals of

Table III. HF Energies of Lithium Cation

basis	energy, hartree
minimal	-7.232 744
split valence	-7.235 984
numerical <sup>a</sup>	-7.236 414 0

<sup>a</sup>See ref 19.

Table IV. Molecular Structure and Energy of Ethene

	basis		expt <sup>a</sup>
	minimal	split val.	
E, hartree	-77.729183	-77.926964	
R <sub>CC</sub> , Å	1.3970	1.3570	1.334
R <sub>CH</sub> , Å	1.1753	1.0869	1.090
$\varphi_{\text{HCH}}$ , deg	116.29	116.56	116.6

<sup>a</sup>See ref 21.

the metal ion will be added to the already mentioned active space (cf. Table II).

The active electrons will be chosen in a manner similar to the choice of the active orbital space. This means ethene will have two active electrons, allyl anion (X) will have four active electrons, and anion I will have six active electrons. The electrons of the metal ion were inactive in the calculations of the ion-pair complexes (see Table II). These choices of active orbitals and active electrons will give a number of CI configurations, as shown in Table II.

The calculations were performed on a FPS array processor with a VAX as front-end. Generation of integrals was done by the MOLECULE program of Almlöf.<sup>13</sup> The CASSCF wave functions were computed by a super-CI-type CASSCF program coded especially for the FPS.<sup>12</sup>

**Analytical Gradients and Relaxation.** It is thought that the bond order can be identified through the equilibrium distance of the interacting atoms. Hence, we will compute structures which are energy minima with respect to the nuclear coordinates. This is, however, not the major reason for using minimized structures. In order to gain coherency between the various complexes with respect to the optimal solution of the wave function within the given constraints of the model and the model parameters, we will need energetically minimized structures. Since the systems which we study are fairly large, we are not able to use as many basis functions on each center as we would have liked. Hence, the equilibrium geometries should not be directly compared to experimental results. In order to establish a new framework for comparison we will compute the structures of some adequate complexes. This framework will, for a given basis, tell us what the wave function, the bond lengths, and the charge distribution look like.

The gradient calculation was performed on a FPS164 by the MOLECULE gradient program of Helgaker.<sup>14</sup> The method of computation has been fully reviewed by Taylor.<sup>15</sup>

The relaxation procedure was performed in an approximate fashion due to the size of the basis sets. The relaxation of the molecules was done by an FPS resident program written by one of the authors (R.L.). The relaxation program uses symmetry-adapted internal coordinates throughout the whole relaxation procedure. This will decrease the number of elements of the force constant matrix as compared to the program

(8) Roos, B.; Siegbahn, P. *Theor. Chim. Acta* **1970**, *17*, 209.

(9) Huzinaga, S. *J. Chem. Phys.* **1965**, *42*, 1293.

(10) (a) Dunning, T. H., Jr. *J. Chem. Phys.* **1970**, *53*, 2823. (b) Dunning, T. H., Jr.; Hay, P. J. In *Methods of Electronic Structure Theory*; Schaefer, H. F., III, Ed.; Plenum: New York, 1977; p 1.

(11) (a) Siegbahn, P.; Helberg, A.; Roos, B.; Levy, B. *Phys. Scr.* **1980**, *21*, 323. (b) Roos, B. O.; Taylor, P. R.; Siegbahn, P. E. M. *Chem. Phys.* **1980**, *48*, 157.

(12) Roos, B. O. *Int. J. Quantum Chem., Quantum Chem. Symp.* **1980**, *14*, 175. A fully vectorized version of the CASSCF super-CI program, adopted to run on FPS-X64 and CRAY, has been written by B. O. Roos and P. E. M. Siegbahn.

(13) Almlöf, J., MOLECULE integral program description. Report 74-29, University of Stockholm, Sweden, Institute of Theoretical Physics, 1974.

(14) Helgaker, T., private communications.

(15) Taylor, P. R. *J. Comput. Chem.* **1984**, *5*, 589.

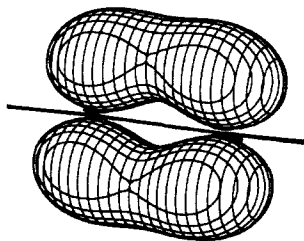


Figure 2. Density plot of the  $\pi$  system of ethene calculated with split-valence basis. Contour surface at 0.02 au.

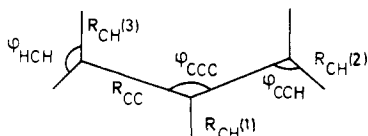


Figure 3. Allyl structure in  $C_{2v}$  symmetry.

Table V. Energy and Molecular Structure of the Allyl Radical in  $C_{2v}$  Symmetry (Split-Valence Basis)

	this work	ref 22f
$E$ , hartree	-116.286559	-116.47259
bonds, Å		
$R_{CC}$	1.4045	1.390
$R_{CH}$ (1)	1.0876	1.078
$R_{CH}$ (2)	1.0870	1.074
$R_{CH}$ (3)	1.0847	1.076
angles, deg		
$\phi_{CCC}$	124.8	124.6
$\phi_{CCH}$	121.3	121.4
$\phi_{HCH}$	117.4	117.6

of Saebo,<sup>16</sup> which uses atomic Cartesian coordinates as a basis. The updating method of the approximate force constant matrix will, however, be of the same type as in the program of Saebo.<sup>16</sup>

For anion I calculated with the split-valence basis the CH distances were constrained to 1.08 Å. For all other relaxations all degrees of freedom were varied. The norm of the atomic Cartesian gradient vector<sup>17</sup> was used as a measure of how close a molecular structure was to the true minima of the potential surface. All relaxations were continued until the size of the norm of the gradient was of the same order of magnitude as the error of the gradient vector.<sup>18</sup>

## Results

**Lithium Cation.** The lithium cation has been investigated at the Hartree-Fock (HF) level of theory. This is consistent with the idea that lithium lends its p orbitals to the anion, keeping its own 1s electrons. The HF results (see Table III) are in agreement with the numerical HF value presented by Clementi et al.<sup>19</sup>

**Ethene.** The energy-minimized structure of ethene in planar symmetry is presented in Table IV. A striking difference between the results of this paper and earlier HF calculations<sup>20</sup> of ethene is the elongation of the CC bond distance. This is, however, not surprising since the CASSCF wave function correlates the  $\pi-\pi^*$  interaction. In comparison to the experimental results of Kuchitsu<sup>21</sup> the HF calculations give a too short CC bond distance and the CASSCF results give a too long distance. The advantage of the CASSCF method, however, is the better representation of

(16) Saebo, S., MOLFORC program description, Technical Report, University of Oslo, Norway, 1979.

(17) An atomic Cartesian gradient vector is a Cartesian gradient vector which also contains elements which are redundant due to symmetry; i.e., the gradient vector of water has nine elements and not three elements.

(18) If the norm of the gradient vector is divided by the number of components, the result will indicate the average gradient at a center in any direction. This average will at the end of the relaxation be of the same order of magnitude as the accuracy of a gradient component.

(19) Clementi, E.; Roetti, C. *At. Data Nucl. Data Tables* **1974**, *14*, 177.

(20) Bock, C. W.; George, P.; Mains, G. J.; Trachtman, M. *J. Mol. Struct.* **1978**, *49*, 215.

(21) Kuchitsu, K. *J. Chem. Phys.* **1966**, *44*, 906.

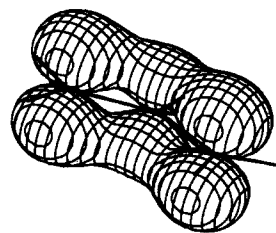


Figure 4. Density plot of the  $\pi$  system of allyl anion (X) calculated with split-valence basis. Contour surface at 0.02 au.

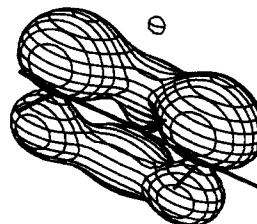


Figure 5. Density plot of the  $\pi$  system of allyllithium calculated with split-valence basis. Contour surface at 0.02 au.

the wave function. The density plot of the  $\pi$  system (the active orbital space) of the molecule is presented in Figure 2.

**Allyl Anion, Allyl Radical, and Allyllithium.** The calculations were performed by using both basis sets, except for the allyl radical which was only computed with a split-valence basis. The internal coordinates for the allyl radical and allyl anion (X) in  $C_{2v}$  symmetry are shown in Figure 3.

In comparison with HF calculations, where similar basis sets have been used, we should expect a lower total energy and somewhat longer bond distances. In comparison with earlier theoretical studies<sup>22</sup> good agreement was found as presented in Tables V-VII.

The electronic structure of the  $C_3$  carbanionic  $\pi$  system is of great interest in anion I. The density plots of the  $\pi$  system of the allyl anion (X), in the absence and presence of lithium cation, are presented in Figures 4 and 5. The density plot readily demonstrates that the charge is localized in the presence of the lithium cation. From our calculations we conclude that the structure of the  $C_3$  carbanionic bridge of anion I will change considerably on interaction with the lithium cation. This change is due to the electrostatic interaction of the hydrogens, the lithium cation, and the  $\pi$  electrons of the carbons. It is reasonable to assume that a similar change in anion I will be somewhat inhibited by the ring constraints. The calculations at this stage also tell us that any change in the charge distribution of the allyl anion (X) will have minor effects on the length of the CC bond distances which are 1.4045 and 1.4066 Å for the radical and anion, respectively, with split-valence basis. Thus, a delocalization of the charge will produce only a small change of the  $C_3$  carbanionic CC bond distance.

**Bicyclooctadienyl Anion and Bicyclooctadienyllithium.** The wave function will at this stage be analyzed with respect to the CI configurations, the Mulliken charge distributions, the density plots of the active orbital space, and the molecular structures.

In the case of bishomoaromaticity, CI configurations corresponding to  $\pi(C_2 \text{ olefinic})-\pi^*(C_3 \text{ carbanionic})$  excitation and

(22) (a) Bongini, A.; Cainelli, G.; Cardillo, G.; Palmieri, P.; Umani-Ronchi, A. *J. Organomet. Chem.* **1976**, *110*, 1. (b) Boerth, D. W.; Streitwieser, A., Jr. *J. Am. Chem. Soc.* **1978**, *100*, 750. (c) Cremaschi, P.; Moros, G.; Simonetta, M.; *THEOCHEM* **1981**, *85*, 397. (d) Decher, G.; Boche, G. *J. Organomet. Chem.* **1983**, *259*, 31. (e) Clark, T.; Rodhe, C.; Schleyer, P. v. R. *Organometallics* **1983**, *2*, 1344. (f) Schleyer, P. v. R. *J. Am. Chem. Soc.* **1985**, *107*, 4793. (g) Clark, T.; Jemmis, E. D.; Schleyer, P. v. R.; Binkley, J. S.; Pople, J. A. *J. Organomet. Chem.* **1978**, *150*, 1.

(23) Jonsäll, G. *Abstract of Uppsala Dissertations from the faculty of Science*, Acta Universitatis Upsaliensis, 1984; Vol. 722.

(24) Setzer, W. N.; Schleyer, P. v. R. *Adv. Organomet. Chem.* **1985**, *24*, 374.

(25) Goldstein, M. J.; Tomoda, S.; Whittaker, G. *J. Am. Chem. Soc.* **1974**, *96*, 3676.

Table VI. Energies and Molecular Structures of Allyl Anion in  $C_{2v}$  Symmetry

	basis		ref 22a	ref 22b	ref 22f
	minimal	split-val.			
$E$ , hartree	-116.007070	-116.234172	-116.2258 <sup>a</sup>	-116.226032	-116.42520
bonds, Å					
$R_{CC}$	1.4267	1.4066	1.390	1.382	1.388
$R_{CH}$ (1)	1.1772	1.0992	1.08 <sup>b</sup>	1.08 <sup>b</sup>	1.087
$R_{CH}$ (2)	1.1557	1.0925	1.08 <sup>b</sup>	1.08 <sup>b</sup>	1.078
$R_{CH}$ (3)	1.1578	1.0904	1.08 <sup>b</sup>	1.08 <sup>b</sup>	1.080
angles, deg					
$\varphi_{CCC}$	132.7	132.1	132.2	132.8	132.2
$\varphi_{CCH}$	121.4	120.9	120.0 <sup>b</sup>	120.0 <sup>b</sup>	120.8
$\varphi_{HCH}$	116.7	117.2	120.0 <sup>b</sup>	120.0 <sup>b</sup>	117.3

<sup>a</sup> Interpolated from table. <sup>b</sup> Fixed.Table VII. Energies and Molecular Structures of Allyllithium Complex in  $C_s$  Symmetry

	basis			<i>a</i>	<i>b</i>	<i>c</i>
	minimal	split-val.				
$E$ , hartree	-123.516448	-123.754227		-122.39929		-123.22823
bonds, Å						
$R_{CC}$	1.4375	1.4166		1.401	1.426	1.393
$R_{CH}$ (1)	1.1709	1.0910		1.090	1.102	
$R_{CH}$ (2)	1.1569	1.0855		1.075	1.095	
$R_{CH}$ (3)	1.1578	1.0961		1.084	1.111	
$R_{CLi}$ (1)	2.1218	2.1311		2.006	2.056	2.093
$R_{CLi}$ (2)	2.1963	2.1796		2.039	2.087	2.141
angles, deg						
$\varphi_{CCC}$	127.5	126.3		123.0	123.9	125.9
$\varphi_{CCH}$	120.5	119.5		118.6	118.8	
$\varphi_{HCH}$	115.4	114.9			120.9	
out of CCC plane angles (positive toward lithium), deg						
$\varphi_H$ (1)	10.5	11.9		11.1	7.4	11.3
$\varphi_H$ (2)	0.8	-0.5		-3.0	1.0	1.0
$\varphi_H$ (3)	-21.7	-24.8		-31.1	-29.2	-28.1

<sup>a</sup> SCF and STO-3G, see ref 22g. <sup>b</sup> MNDO, see ref 22d. <sup>c</sup> SCF and 3-21G, see ref 22e.Table VIII.  $CH_x$  Mulliken Charge Distribution

complex	ethene CH	allyl		top $CH_2$	bridge CH
		CH	$CH^a$		
Minimal Basis					
$C_2H_4$	-0.156				
$C_3H_5^-$		-0.437	-0.157		
$LiC_3H_5$		-0.411	-0.149		
$C_8H_9^-$	-0.072	-0.252	-0.147	-0.049	-0.079
$LiC_8H_9$	-0.102	-0.204	-0.178	+0.010	-0.041
Split-Valence Basis					
$C_2H_4$	-0.136				
$C_3H_5^-$		-0.474	-0.112		
$C_3H_5$		-0.002	+0.004		
$LiC_3H_5$		-0.367	-0.011		
$C_8H_9^-$	-0.066	-0.287	-0.087	-0.002	-0.102

<sup>a</sup> Middle carbon.

nonbonding  $\pi(C_3$  carbanionic)– $\pi^*(C_2$  olefinic) excitation would have large CI coefficients. This is, however, not the case for anion I with the two basis sets and the anion I lithium cation complex. Here the wave functions were 90%, 92%, and 89% HF ground-state character. The rest of the configurations with large coefficients were excitations within the  $C_2$  olefinic or the  $C_3$  carbanionic bridge of the anion. The nonaromatic excitations corresponded to 8%, 7%, and 7% of the wave function for anion I with the two basis sets and the anion I lithium cation complex, respectively. Excitations indicating aromatic character were less than 2–3% in all wave functions.

The Mulliken charge distribution will give some hints about the delocalization of the charge. The  $CH_x$  and the carbon charges are presented in Tables VIII and IX, respectively. For the split-valence basis the charge of the allyl termini in the allyl anion,  $q(C) = -0.504$ , is to some extent delocalized in anion I,  $q(C) = -0.327$ . The charges of the middle carbon,  $q(C) = -0.096$  and  $q(C) = -0.117$ , for the allyl anion (X) and anion I, respectively,

Table IX. Carbon Mulliken Charge Distribution

complex	ethene C	allyl		top C	bridge C
		C	$C^a$		
Minimal Basis					
$C_2H_4$	-0.311				
$C_3H_5^-$		-0.452	-0.215		
$LiC_3H_5$		-0.495	-0.282		
$C_8H_9^-$	-0.168	-0.288	-0.215	-0.272	-0.180
$LiC_8H_9$	-0.232	-0.314	-0.298	-0.288	-0.198
Split-Valence Basis					
$C_2H_4$	-0.273				
$C_3H_5^-$		-0.504	-0.096		
$C_3H_5$		-0.289	-0.124		
$LiC_3H_5$		-0.516	-0.132		
$C_8H_9^-$	-0.130	-0.327	-0.117	-0.134	-0.108

<sup>a</sup> Middle carbon.

are almost the same. The same result is true for the minimal basis calculations. Furthermore, in the anion I lithium cation complex there is just a minor change in the charge compared to anion I. However, as expected the charge is polarized toward the lithium cation (see Figure 5). For the  $C_2$  olefinic bridge of anion I, the Mulliken population analysis indicates a loss of charge. The energy-minimized structures (see Tables X and XI) show that the  $C_2$  olefinic and the  $C_3$  carbanionic bridges are almost perpendicular to each other. If there were a bishomoaromatic interaction, this would only be possible were the lobes of the p orbitals pointing toward each other. Hence, the charge would be delocalized in this region. However, the charge is localized in the bridging part of the molecule; i.e., the charge distribution is not typically aromatic.

The density plots for the orbitals of the active orbital space of anion I, calculated with the split-valence basis, show that there is a very small interaction between the  $C_3$  carbanionic orbitals and the  $C_2$  olefinic orbitals (see Figure 6). The occupied orbitals

**Table X.** Molecular Structure of Anion I and the Anion I Lithium Cation Complex in *C<sub>s</sub>* Symmetry

	<i>a</i>	<i>b</i>	<i>c</i>	<i>d</i>
<i>E</i> , hartree	-304.22064	-307.056450	-307.525846	-314.558658
CC bonds, Å				
C <sub>1</sub> -C <sub>2</sub>	1.558	1.551	1.529	1.560
C <sub>2</sub> -C <sub>3</sub>	1.395 <sup>f</sup>	1.425	1.408	1.435
C <sub>1</sub> -C <sub>7</sub>	1.533	1.563	1.537	1.567
C <sub>1</sub> -C <sub>8</sub>	1.565	1.581	1.557	1.580
C <sub>2</sub> -C <sub>7</sub>	2.543	2.470	2.461	2.512
C <sub>2</sub> -C <sub>8</sub>	2.540	2.545	2.513	2.550
C <sub>6</sub> -C <sub>7</sub>	1.356 <sup>e</sup>	1.397	1.370	1.395
CLi bonds, Å				
C <sub>3</sub> -Li				2.120
C <sub>2</sub> -Li				2.296
CH bonds, Å				
C <sub>1</sub> -H	1.09 <sup>g</sup>	1.169	1.080 <sup>g</sup>	1.169
C <sub>2</sub> -H	1.09 <sup>g</sup>	1.151	1.080 <sup>g</sup>	1.154
C <sub>3</sub> -H	1.09 <sup>g</sup>	1.168	1.080 <sup>g</sup>	1.162
C <sub>6</sub> -H	1.09 <sup>g</sup>	1.163	1.080 <sup>g</sup>	1.159
C <sub>8</sub> -H (anti)	1.09 <sup>g</sup>	1.171	1.080 <sup>g</sup>	1.171
C <sub>8</sub> -H (syn)	1.09 <sup>g</sup>	1.168	1.080 <sup>g</sup>	1.169

<sup>a</sup>MNDO calculation, see ref 5b. <sup>b</sup>Minimal basis. <sup>c</sup>Split-valence basis. <sup>d</sup>Bicyclooctadienyllithium, minimal basis. <sup>e</sup>Extrapolated from table. <sup>f</sup>Misprint in ref 5b, 1.517 is wrong. <sup>g</sup>Fixed in the relaxation.

**Table XI.** Additional Geometric Variables in Anion I and the Anion I Lithium Cation Complex

	<i>a</i>	<i>b</i>	<i>c</i>
bond angles, deg			
C <sub>1</sub> -C <sub>8</sub> -C <sub>5</sub>	100.4	99.9	100.1
C <sub>1</sub> -C <sub>2</sub> -C <sub>3</sub>	116.0	116.5	116.0
H-C <sub>1</sub> -C <sub>8</sub>	113.1	113.3	113.8
H-C <sub>1</sub> -C <sub>2</sub>	113.5	112.6	112.3
H-C <sub>2</sub> -C <sub>1</sub>	120.6	120.8	120.0
H-C <sub>6</sub> -C <sub>7</sub>	126.7	125.7	127.7
H-C <sub>8</sub> -H	110.1	109.7	109.4
plane angles <sup>d</sup> (>180° toward Li), deg			
C <sub>8</sub> -C <sub>1</sub> -C <sub>5</sub> -C <sub>4</sub>	117.7	118.1	117.4
C <sub>1</sub> -C <sub>2</sub> -C <sub>4</sub> -C <sub>3</sub>	182.3	181.1	166.2
C <sub>7</sub> -C <sub>1</sub> -C <sub>5</sub> -C <sub>8</sub>	137.0	134.8	135.2
out-of-plane angles <sup>e</sup> (positive toward C <sub>8</sub> ), deg			
H-C <sub>3</sub> -C <sub>2</sub> -C <sub>4</sub>	-1.6	-1.3	-6.3
H-C <sub>2</sub> -C <sub>4</sub> -C <sub>1</sub>	-2.3	-2.1	9.7
H(syn)-C <sub>8</sub> -C <sub>1</sub> -C <sub>5</sub>	54.1	53.4	52.5
H-C <sub>6</sub> -C <sub>5</sub> -C <sub>7</sub>	-9.8	-12.8	-3.0

<sup>a</sup>Minimal basis. <sup>b</sup>Split-valence basis. <sup>c</sup>Bicyclooctadienyllithium, minimal basis. <sup>d</sup>The angles between plane 123 and plane 234. <sup>e</sup>The angle between vector 12 and plane 234.

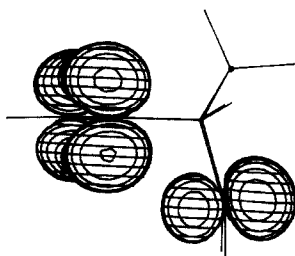


**Figure 6.** Density plot of the active orbital space in the bicyclooctadienyl anion computed with split-valence basis. Contour surface at 0.02 au.

of the active orbital space are localized C<sub>3</sub> carbanionic  $\pi$  and localized C<sub>2</sub> olefinic  $\pi$ . The density plot even indicates that electrons in the C<sub>2</sub> olefinic  $\pi$  orbital are repelled by the C<sub>3</sub> carbanionic bridge. This can be seen from the shape of the  $\pi$  orbitals of the C<sub>2</sub> olefinic bridge. This polarization is facilitated by a rehybridization of the carbons (C<sub>6</sub>, and C<sub>7</sub>). The rehybridization is readily shown by the CH out-of-plane angle, which is -9.8° and -3.0° in anion I and anion I lithium cation complex, respectively (compare Figures 6 and 7). Furthermore, the polarization of anion I by the lithium cation is shown not to affect the interaction between the two bridges to any large extent. Instead, it reveals that the C<sub>3</sub> carbanionic bridge forms an ion

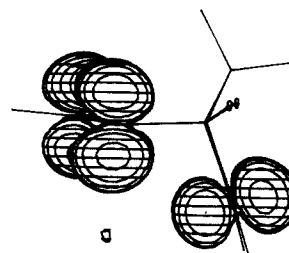


**Figure 7.** Density plot of the active orbital space in bicyclooctadienyl-lithium computed with minimal basis. Contour surface at 0.02 au.

**Table XII.** X-ray Data vs. Semiempirical and ab Initio Results<sup>a</sup>

bonds	X-ray <sup>a</sup>		semiempirical <sup>b</sup>		ab initio <sup>c</sup>	
	<i>r<sub>e</sub></i>	<i>r<sub>e</sub></i>	<i>r<sub>se</sub></i>	<i>r<sub>se</sub> - r<sub>e</sub><sup>d</sup></i>	<i>r<sub>ai</sub></i>	<i>r<sub>ai</sub> - r<sub>e</sub><sup>d</sup></i>
C <sub>1</sub> -C <sub>2</sub>	1.520	1.518	1.558	0.039	1.529	0.010
C <sub>2</sub> -C <sub>3</sub>	1.395	1.384	1.395	0.006	1.408	0.019
C <sub>1</sub> -C <sub>8</sub>	1.542	1.538	1.565	0.025	1.557	0.017
C <sub>1</sub> -C <sub>7</sub>	1.509	1.512	1.533	0.023	1.537	0.027
C <sub>6</sub> -C <sub>7</sub>		1.354	1.356	0.002	1.370	0.016
plane angles	$\varphi_e$	$\varphi_{se}$	$\varphi_{se} - \varphi_e$	$\varphi_{ai}$	$\varphi_{ai} - \varphi_e$	
C <sub>8</sub> -C <sub>1</sub> -C <sub>5</sub> -C <sub>4</sub>	119.2	117.0 <sup>f</sup>	-2.2	118.1	-1.1	
C <sub>7</sub> -C <sub>1</sub> -C <sub>5</sub> -C <sub>8</sub>	137.6	131.9 <sup>f</sup>	-5.7	134.8	-2.8	
C <sub>7</sub> -C <sub>1</sub> -C <sub>5</sub> -C <sub>4</sub>	103.2	111.1 <sup>f</sup>	7.9	107.1	3.9	

<sup>a</sup>Anion I lithium cation TMEDA complex, see ref 26. <sup>b</sup>Anion I, see ref 5b. <sup>c</sup>Anion I calculated with split-valence basis set. <sup>d</sup>In case of asymmetry the difference is calculated from the mean average of the experimental values. <sup>e</sup>Bond distances are in Å; plane angles are in degrees. <sup>f</sup>Anion I lithium cation complex, see ref 28.

pair with the lithium cation (see Figure 7). Hence, the density plots show that bishomoaromaticity in anion I is negligible and that interaction with a lithium cation will not promote bishomoaromaticity.

For the geometrical findings (see Tables X and XI) we will compare some bonds of interest with the bonds in ethene and allyl anion (X) (see Tables IV, VI, and VII). The C<sub>2</sub> olefinic bond distances in ethene are 1.397 and 1.357 Å for a minimal basis and split-valence basis, respectively, whereas the C<sub>2</sub> olefinic bond distances are 1.397 and 1.370 Å in anion I. The C<sub>2</sub> olefinic bond distance is unchanged for the minimal basis. The more diffuse split-valence basis gives just a minor change of the bond distance. This elongation could correspond to some interaction between the C<sub>2</sub> olefinic  $\pi^*$  orbital and another orbital, e.g., the C<sub>3</sub> carbanionic nonbonding orbital. However, the change of the bond distance of the C<sub>2</sub> olefinic bond is more likely to be due to the ring constraints. The interaction with lithium cation does not affect the C<sub>2</sub> olefinic bond distance. For the C<sub>3</sub> carbanionic bond distance (1.427 and 1.407 Å in the allyl anion (X) with minimal basis and split-valence basis, respectively) there is almost no change (1.425 and 1.408 Å) in the anion I. However, we can detect a change of the bond distance in the presence of lithium cation. The change in this case is very similar to the change from allyl anion (X) to allyllithium. In both cases the bond distance is increased by 0.01 Å, and furthermore, the out-of-plane angles of the hydrogens (H<sub>2</sub>, H<sub>3</sub>, and H<sub>4</sub>) are distorted in a way which is very similar to the allyllithium complex. Finally, we can observe that upon interaction with the lithium cation, the C<sub>3</sub> carbanionic bridge bends away by 16.1° (see Figures 6 and 7). This distortion will promote the interaction between the lithium cation and the C<sub>2</sub> olefinic bridge and decreases the overlap between the  $\pi$  systems of the C<sub>3</sub> carbanionic bridge and the C<sub>2</sub> olefinic bridge.

The above analysis of anion I and the anion I lithium complex does not exhibit any interaction of importance between the two  $\pi$  systems. The X-ray data of the asymmetrical anion I lithium cation TMEDA complex<sup>26</sup> as well as the computation of the anion I lithium cation complex at the MNDO level of theory<sup>28</sup> reached us at the time of finishing this paper. The experimental results

(26) Hertkorn, N.; Köhler, F. H.; Müller, G.; Reber, G. *Angew. Chem., Int. Ed. Engl.* **1986**, *25*, 468.

give us a possibility to establish the quality of our calculations. The results are compared with both semiempirical and ab initio results (see Table XII). To compare the geometries of different complexes of anion I may seem invalid. However, the geometry of anion I does not change significantly, with respect to the bond distances and plane angles, under complexation as shown earlier in this paper. As we can see, there is an excellent agreement between experimental and theoretical findings. Furthermore, the experimental results support our conclusions since the C<sub>6</sub>–C<sub>7</sub> bond distance of 1.354 Å indicates no presence of homoaromatic stabilization in anion I.

**Ethene and Lithium Cation.** The complex of ethene and lithium cation has been investigated at the SCF level of theory. In the calculation with minimal basis the ethene–lithium cation complex was configured in the same way as it occurs in the fully relaxed anion I lithium cation complex. In this configuration the lithium cation is positioned at a distance of 2.27 Å to the center of the CC bond and almost perpendicular to the plane of the ethene molecule. For this configuration the energy of stabilization was 18.0 kcal/mol and the energy of stabilization corrected for basis set superposition error (BSSE) was 9.8 kcal/mol. With the split-valence basis, the same position of the lithium cation relative to the ethene molecule was chosen. However, the structure of the ethene molecule was chosen as in the relaxed ethene molecule with split-valence basis. This resulted in an energy of stabilization of 16.4 and 16.2 kcal/mol, respectively, for the noncorrected and the BSSE-corrected energies. Both results indicate a considerable stabilization of the ethene–lithium cation complex. It is reasonable to assume this interaction to be the same in the complex of anion I and the lithium cation. Thus, when anion I forms a complex with the lithium cation a major contribution to the stabilization comes from the C<sub>3</sub> carbanionic bridge (about 135 kcal/mol), and a minor contribution comes from the C<sub>2</sub> olefinic bridge (about 16 kcal/mol).

**Binding Energies and BSSE.** The binding energy of the anion I lithium cation complex has been compared to the binding energy of allyllithium. If the binding energies are of the same size, this would indicate a similarity in the interaction of the two complexes. This is the case since the binding energy difference depends on the localization of the negative charge in anion I as compared to the allyl anion (X). The binding energies were found to be 173.6 and 169.1 kcal/mol for allyllithium and the anion I lithium cation complex, respectively. The binding energy was also analyzed with respect to BSSE. This was done by subtracting the energy gains due to the difference in basis sets between the calculations. This gives us binding energies of 157.5 and 149.2 kcal/mol for allyllithium and the anion I lithium cation complex, respectively. Thus, the BSSE is about 10% the total energy difference. The calculated binding energies are in line with the earlier finding that anion I largely resembles a noninteracting ethene and allyl anion. Hence, no bishomoaromaticity is found in the anion.

## Discussion

**Bicyclooctadienyl Anion I.** This apparently important example of anionic homoaromaticity<sup>4</sup> has been reinvestigated on the CASSCF level of theory. The results obtained concerning geometry, charge distribution, electron density, and CI configurations have definitely ruled out any significant contribution of homoaromatic features to the structure of anion I.

On the contrary, we found negative charge to be delocalized primarily through bonds to all parts of the carbon skeleton (Tables VIII and IX) rather than transferred through space to C<sub>6</sub> and C<sub>7</sub>, which were found to be less negative than the carbons of ethene. We also revealed a considerable rehybridization of C<sub>6</sub> and C<sub>7</sub> tilting H<sub>6</sub> and H<sub>7</sub> 9.8° out of plane, *diminishing* the overlap between the π systems of the C<sub>2</sub> olefinic bridge and the C<sub>3</sub> carbanionic bridge.

Our results confirm the conclusions of Grutzner and Jorgensen and Kaufmann et al.<sup>5a,b</sup> regarding the unimportance of homoaromatic interactions among bicyclic carbanions. However, there is a wealth of experimental data in the literature<sup>4</sup> showing anion I and related structures to have unusual stability and remarkable

spectroscopic properties. How can these data be accounted for?

In a recent gas-phase experiment by Lee and Squires,<sup>27</sup> the energy change for I + III → II + VI was reported to be 9.5 ± 2.0 kcal/mol. On the basis of this result, which is in line with the 12.2 kcal/mol difference measured in cyclohexylamine solution by Washburn,<sup>6</sup> Lee and Squires conclude that bishomoaromaticity is the main cause. However, the quantitative results can just as well be derived from a simple electrostatic model. This model is based on the electrostatic difference of the ethane and ethene molecules. The charge of the C<sub>3</sub> carbanionic bridge was localized at the three centers (C<sub>2</sub>, C<sub>3</sub>, and C<sub>4</sub>) in accordance with the Mulliken population analysis. The experimental quadrupole moments of ethane and ethene were placed at the C<sub>2</sub> olefinic bridge. All geometrical parameters of this charge–quadrupole model were those of anion I calculated with the split-valence basis set. The quadrupole–charge interaction revealed a relative stabilization of the charge in the C<sub>3</sub> carbanionic bridge by 5.8 kcal/mol on going from ethane to ethene. Furthermore, due to the difference in polarizability of ethane and ethene we estimate the relative inductive and dispersive stabilizations both to be around 1 kcal/mol. Thus, the total relative stability on going from ethane to ethene adds up to around 8 kcal/mol, which is in agreement with experimental findings.<sup>27</sup>

**Bicyclooctadienyllithium.** In an investigation of ion VII we recently suggested<sup>7,23</sup> that the role of the counterion, known to be important in most aspects of carbanion chemistry, had been seriously underestimated in previous work regarding homoaromaticity. This was especially true regarding earlier theoretical studies, which all treated the isolated anions.<sup>5</sup>

We assumed the lithium cation to occupy a bridging position between the C<sub>3</sub> carbanionic bridge and the C<sub>2</sub> olefinic bridge. In our original hypothesis we then expected lithium p orbitals to serve as a conductor between the different bridges, allowing negative charge to flow into the C<sub>2</sub> olefinic bridge. This idea has now been explored in CASSCF calculations with a minimal basis set.

A lithium cation was introduced together with anion I, and the complex was completely geometry optimized, giving some interesting results. The geometrical changes are most prominent within the C<sub>3</sub> carbanionic bridge. Upon complexation with lithium cation the C<sub>3</sub> carbanionic bridge is tilted away from the C<sub>2</sub> olefinic bridge. Such deformations are well-known from the allyllithium ion pair and considered to be electrostatic in origin.<sup>22b,24</sup> Here they will serve to further decrease eventual homoaromatic interactions.

The C<sub>3</sub> carbanionic bond length (C<sub>2</sub>–C<sub>3</sub>) was found to increase by 0.01 Å, while C<sub>6</sub>–C<sub>7</sub> remained practically unchanged in length. However, the out-of-plane tilting of H<sub>6</sub>–H<sub>7</sub> is decreased to –3°, leaving a rather symmetric electron distribution around the double bond. This rehybridization placed lithium cation, while still complexed to C<sub>2</sub>–C<sub>3</sub>–C<sub>4</sub>, almost perpendicular to the C<sub>6</sub>–C<sub>7</sub> double bond on the axis of highest electron density (Figure 7).

Charge distributions underwent some minor changes, transferring some charge from C<sub>2</sub>–C<sub>4</sub> to other positions. However, this charge goes almost equally to all other positions rather than being directed specifically toward C<sub>6</sub>–C<sub>7</sub> (Tables VIII and IX). All these results, when taken together, indicated that the lithium cation attenuated rather than promoted homoaromatic interactions.

**Ethene and Lithium Cation.** Complementary calculations with ethene and lithium cation fixed at the distance found in the anion I lithium cation complex revealed a large interaction stabilizing this complex by as much as 16 kcal/mol. A considerable involvement of ethene orbitals was also indicated in the spectroscopic studies of VII, which found the C–H coupling constants (<sup>1</sup>J<sub>C–H<sub>6</sub>) to be 25 Hz less in VII than in the corresponding hydrocarbon IV.<sup>7,23,25</sup> However, the counterion–anion interaction as well as the charge–quadrupole interaction and the inductive stabilization are sensitive to shielding from the solvent. Thus, the different contributions should not simply be added up but rather accounted for in respect to the type of solvent which is used and the degree</sub>

(27) Lee, R. E.; Squires, R. R. *J. Am. Chem. Soc.*, in press.

(28) Schleyer, P. v. R.; Kaufmann, E.; Kos, A. J. *J. Chem. Soc., Chem. Commun.*, in press.

of complexation of the counterion. This extra stabilization from the counterion and the shielding effects give us a possible explanation of the difference between the gas-phase result and the solution result.

Our original hypothesis of a charge relay from the C<sub>3</sub> carbanionic bridge to the C<sub>2</sub> olefinic bridge in anion I via lithium p orbitals has not found support in these calculations. True, the lithium cation was found to occupy the proposed position between the  $\pi$  systems of the two bridges, but its interaction is mostly electrostatic in nature. The rehybridization of C<sub>6</sub> and C<sub>7</sub>, the coordination of these carbons with the lithium cation, and a considerable redistribution of charge through bonds might be responsible for the unusual NMR spectral properties of I.<sup>4</sup>

### Conclusion

The results obtained in the present study do not give any indication that bishomoaromaticity is an important factor in the chemistry of anion I and related carbanions. Rather, it seems possible to explain the 30-year-old controversy<sup>1</sup> in terms of the quadrupolar property of the C<sub>2</sub> olefinic bridge in anion I and the role of the counterion in solution. Such explanations have not

been considered in earlier work.

It may be argued that this study is too primitive to allow firm conclusions to be drawn. Notably, the basis sets used in the calculations are rather limited, and it has only been possible to account for the most important part of the correlation effects, the near degeneracy correlation in the  $\pi$  system of the carbanion. Even if calculations using larger basis sets (especially including diffuse 2p-type functions on the carbon atoms in the allylic bridge) would be of value, we do not believe that the results would be very different from those obtained in the present study. The net interaction between the allylic and the olefinic part of the ion would still be repulsive rather than attractive.

**Acknowledgment.** We acknowledge helpful discussions with Prof. P. v. R. Schleyer and docent Gunnar Karlström. We are also grateful to E. Kaufmann, R. R. Squires, F. H. Köhler, and P. v. R. Schleyer for providing us with their manuscripts prior to publication. This project was supported by a grant from the Swedish Natural Science Research Council (NFR).

**Registry No.** C<sub>2</sub>H<sub>4</sub>, 74-85-1; C<sub>3</sub>H<sub>5</sub>, 1981-80-2; C<sub>3</sub>H<sub>5</sub><sup>-</sup>, 1724-46-5; LiC<sub>3</sub>H<sub>5</sub>, 3052-45-7; C<sub>8</sub>H<sub>9</sub><sup>-</sup>, 76881-29-3; LiC<sub>8</sub>H<sub>9</sub>, 101671-14-1.

## Electronic Structure of Transition-Metal Borides with the AlB<sub>2</sub> Structure

Jeremy K. Burdett,\* Enric Canadell,<sup>†</sup> and Gordon J. Miller

Contribution from the Department of Chemistry, The University of Chicago, Chicago, Illinois 60637. Received April 9, 1986

**Abstract:** A study of the electronic structure of solid metal borides with the AlB<sub>2</sub> structure type is presented. The interaction of the orbitals of the transition metal with those of a planar, graphite-like net of boron atoms and the interaction with those of other metals are both important in influencing the properties of these species. It is suggested that the experimentally observed variation in the heat of formation of these species is crucially dependent upon the extent of occupation of the metal-boron orbital set. In addition it appears that the puckering of the boron net in ReB<sub>2</sub> and RuB<sub>2</sub> structures is due not to the obvious effects of charge transfer but to strong metal-metal repulsions perpendicular to the nonmetal sheets. In AlB<sub>2</sub> itself the strongest interactions are between the boron atoms which attain a graphite-like electron count with its associated structural stability.

The AlB<sub>2</sub> structure<sup>1</sup> is one which is adopted by many of the transition-metal diborides (Table I). It may be regarded (Figure 1) as a completely intercalated graphite in the sense that all of the hexagonal prismatic sites of the primitive graphite structure are filled. The empty primitive lattice is unknown for carbon itself but is found for the derivative BN. (In carbon adjacent sheets are displaced with respect to each other.) Derivative AlB<sub>2</sub> systems are also known, NaBeAs is an example, where the 6<sup>3</sup> nets contain alternatively Be and As. In several of the examples with this structure, such as MgB<sub>2</sub>, CaGa<sub>2</sub>, and NaBeAs, if electron transfer from the intercalated atom to the sheet is assumed to be complete, then the sheet itself is isoelectronic with graphite or a heavier group 14 analogue (B<sup>-</sup>, Ga<sup>-</sup>, BeAs<sup>-</sup>). Addition of electrons leads to a nonplanar sheet, CaSi<sub>2</sub>, for example (Figure 2), contains puckered silicon sheets, just like those found in the structures of elemental As, Sb, and Bi. Si<sup>-</sup> is, of course, isoelectronic with the group 15 elements. Transition-metal diborides with the AlB<sub>2</sub> structure are known for the first-row elements Sc through Mn. Obviously here there is not complete electron transfer from the metal to the boron sheet. For the second- and third-row transition-metal series a changeover in structure occurs between groups 6 and 7 and between 7 and 8. The RuB<sub>2</sub> structure is one composed of puckered graphite sheets and is related<sup>2</sup> to the structure of "tetragonal

Table I. Occurrence of Borides with the AlB<sub>2</sub> or Related Structures

Mg								
X								
Ca	Sc	Ti	V	Cr	Mn	Fe	Co	Ni
	X	X	X	X	X			
Sr	Y	Zr	Nb	Mo	Tc	Ru	Rh	Pd
		X	X	X	X <sup>a</sup>	X <sup>b</sup>		
Ba	La	Hf	Ta	W	Re	Os	Ir	Pt
		X	X		X <sup>a</sup>	X <sup>b</sup>		

<sup>a</sup>Puckered sheet. <sup>b</sup>Corrugated sheet.

carbon". The mode of puckering is different to that found in CaSi<sub>2</sub>, and the result is perhaps best described as the generation of corrugated sheets. The structure of ReB<sub>2</sub> and TcB<sub>2</sub> (*hP6*) is very similar to that of CaSi<sub>2</sub> (*hR6*) and only differs in the way the puckered sheets are stacked. 1 and 2 show the metal coordination geometry in the structures of AlB<sub>2</sub> and ReB<sub>2</sub>. In the former the metal is 12 coordinate and in the latter 8 coordinate. In this paper we examine the interaction of the metal with the

<sup>†</sup>Present address: Laboratoire de Chimie Théorique, Université de Paris-Sud, Orsay 91405, France.

(1) See, for example: (a) Pearson, W. B. *Crystal Chemistry and Physics of Metals and Alloys*; Wiley: New York, 1972. (b) Aronsson, B.; Lundström, T.; Rundqvist, S. *Borides, Silicides and Phosphides*; Wiley: New York, 1965. (c) *Boron and Refractory Borides*; Matkovich, V. I., Ed.; Springer-Verlag: New York, 1977.

(2) Burdett, J. K.; Canadell, E., unpublished results.